scientific reports

Check for updates

OPEN

Limb, joint and pelvic kinematic control in the quail coping with steps upwards and downwards

Emanuel Andrada[1]✉, Oliver Mothes[2], Heiko Stark[1], Matthew C. Tresch[3], Joachim Denzler[2], Martin S. Fischer[1] & Reinhard Blickhan[4]

Small cursorial birds display remarkable walking skills and can negotiate complex and unstructured terrains with ease. The neuromechanical control strategies necessary to adapt to these challenging terrains are still not well understood. Here, we analyzed the 2D- and 3D pelvic and leg kinematic strategies employed by the common quail to negotiate visible steps (upwards and downwards) of about 10%, and 50% of their leg length. We used biplanar fluoroscopy to accurately describe joint positions in three dimensions and performed semi-automatic landmark localization using deep learning. Quails negotiated the vertical obstacles without major problems and rapidly regained steady-state locomotion. When coping with step upwards, the quail mostly adapted the trailing limb to permit the leading leg to step on the elevated substrate similarly as it did during level locomotion. When negotiated steps downwards, both legs showed significant adaptations. For those small and moderate step heights that did not induce aerial running, the quail kept the kinematic pattern of the distal joints largely unchanged during uneven locomotion, and most changes occurred in proximal joints. The hip regulated leg length, while the distal joints maintained the spring-damped limb patterns. However, to negotiate the largest visible steps, more dramatic kinematic alterations were observed. There all joints contributed to leg lengthening/shortening in the trailing leg, and both the trailing and leading legs stepped more vertically and less abducted. In addition, locomotion speed was decreased. We hypothesize a shift from a dynamic walking program to more goal-directed motions that might be focused on maximizing safety.

Encompassing almost ten thousand species, birds (clade Aves) are the most successful bipeds. Despite their flying abilities, they also represent a valuable study group to understand adaptations to terrestrial locomotion. For example, there are bird species that combine remarkable flying and walking abilities (e.g., waders[1,2]). Other species evolved to live on the ground, losing partially or completely their ability to fly. Within the latter group, encompassing about sixty species, the quail (*Coturnix coturnix*), is representative for the group of small cursorial birds. Like most of this group, the quail prefers grounded running (a running gait without aerial phases) during unrestricted level locomotion[3,4]. In the wild, however, the quail must navigate over complex and unstructured terrains. Locomotion might become non-periodic, altering the kinematic and mechanical demands placed on the neuromechanical control system as compared to level locomotion. Our understanding of how animals' neuromechanical control strategies adapt to these changing demands, despite important progress achieved in the past years, remains elusive.

It is believed that animals combine the intrinsic stability of their body mechanics with their neuronal control to negotiate rough terrains. The assumption is that anticipatory (feedforward) mechanisms pre-adjust limb kinematics and impedance before the leg contacts the ground, to reduce the need for reactive (feedback) response to readapt posture during stance[5–9]. In the last years, two-dimensional neuromechanical studies have tried to bring light to the adaptive mechanisms underlying bipedal uneven locomotion. Their results indicate that humans mainly adjust leg stiffness to maintain dynamic stability[10–13], whereas birds seem to rely on leg actuation and kinematic control[14]. Birds use anticipatory maneuvers to vault upwards in order to avoid excessive crouched postures on an obstacle[14,15]. Similar to humans[16], birds use leg retraction in late swing to regulate landing conditions[14,17], to minimize fluctuations in leg loading during uneven locomotion[18], and to prevent falls[19,20]. Late-swing retraction is

[1]Institute of Zoology and Evolutionary Research, Friedrich-Schiller-University Jena, Jena, Germany. [2]Computer Vision Group, Friedrich-Schiller-University Jena, Jena, Germany. [3]Department of Physiology, Northwestern University, Chicago, IL, USA. [4]Science of Motion, Friedrich-Schiller-University Jena, Jena, Germany. ✉email: emanuel.andrada@uni-jena.de

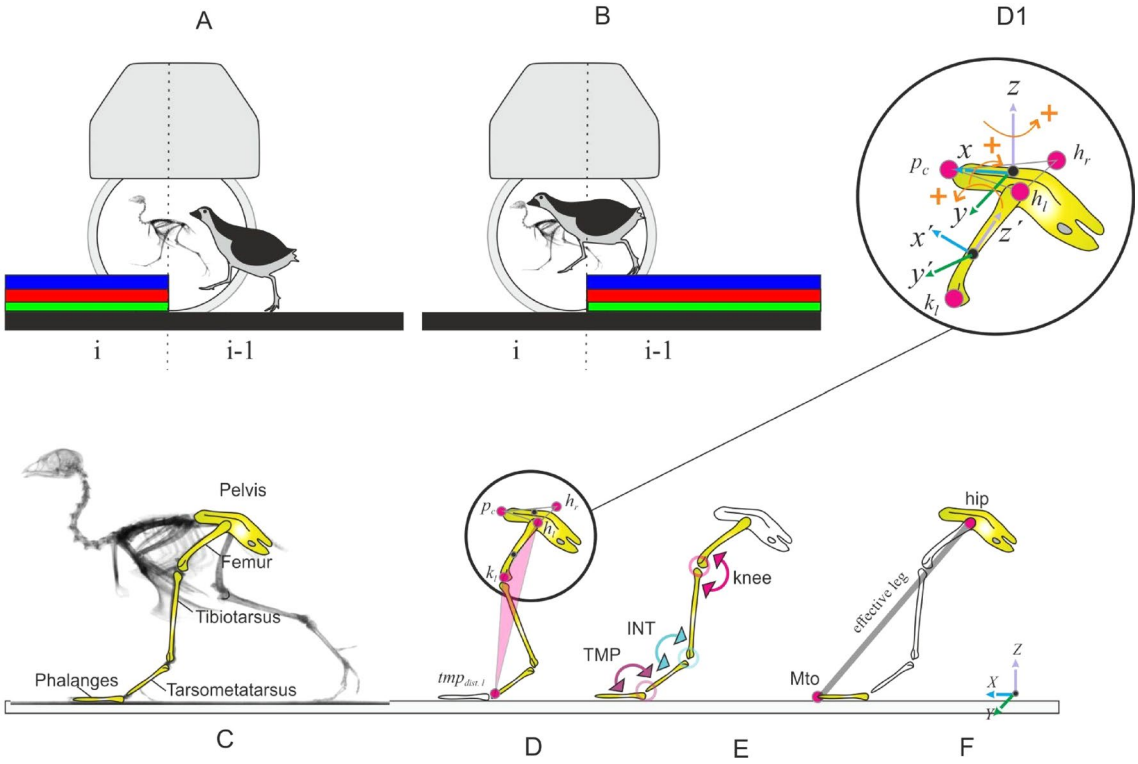

Figure 1. Experimental setup and 2D/3D global and joint limbs kinematics. The quail negotiated visible step-up (**A**) and step-down (**B**) steps of 1 cm (green), 2.5 cm (red), and 5 cm (blue) height. Body and hindlimb kinematics were captured using biplanar fluoroscopy. (**C**) Analyzed body segments. (**D**) 3D kinematics of the pelvis relative to the global coordinate system, and rotation of the whole leg related to the pelvis. The last estimates the three-dimensional rotations occurring at the hip joint. The whole leg is a plane formed by the hip (e.g., h_l), the knee (e.g., k_l) and the distal marker of the tarsometatarsus ($tmt_{dist.\ l}$). Coordinate systems for the pelvis and the leg can be seen in D1, see methods for further explanations, (**E**) joint kinematics (*INT* intertarsal joint, *TMP* tarsometatarsal–phalangeal joint), (**F**) effective leg is the distance between tip of the middle toe (Mto) and the hip.

known to increase stability of locomotion as it changes the angle of attack of the leg at touch down (TD) according to obstacle height[16]. In small birds, the retraction of the leading leg can be the consequence of the leg placement strategy called fixed aperture angle[4]. In this strategy, the angle between the leg going to contact on the ground (usually termed leading) and the supporting legs (usually termed trailing) is fixed before TD. The retraction of the leading leg is thus automatically adapted for locomotion speed[4,21,22]. The aperture angle strategy has not yet been tested in birds facing perturbations, although there is some evidence for its use by humans during uneven locomotion[23]. Simple leg control strategies like the aperture angle might reduce, to some extent, the necessity of anticipatory maneuvers when negotiating light uneven terrains. The robustness of avian level locomotion was also assessed using a simple model including an effective leg (the segment spanning from the hip to the toe, Fig. 1F) and a trunk[22]. The model produced self-stable gaits and was able to cope with steps over obstacles or sudden drops without the need for feedback control or even the need for tuning feedforward strategies[22,24].

To our knowledge, there is no previous literature on three-dimensional analyses of avian locomotion over uneven surfaces. Even for level locomotion, three-dimensional analyses of avian locomotion are uncommon e.g.,[25–28]. However, a three-dimensional analysis is mandatory to address topics like lateral stabilization or navigation control, especially on uneven terrains. Finally, to have a more general picture of the strategies to negotiate uneven terrains, it is important to link the kinematic control occurring at different levels of abstraction (e.g., simple model representations of the leg vs. joint kinematics).

Simple model representations like the effective leg help to understand basic strategies for stability or economy of locomotion e.g.,[4,5,21,29–31] and can be used as global goals for the control of limb joints[32]. During unrestricted locomotion, there is evidence of an interplay between effective leg and limb segmental angles. In humans, Japanese macaques and the quail, limb segmental angles (thigh, shank, and foot) measured in the sagittal plane covary in a way that they form a planar loop in a three-dimensional space[33–37]. This result indicates that intersegmental coordination might reduce the number of degrees of freedom to control the leg from three (i.e., joint angles) to two (i.e., effective leg length and angle).

Due to the redundant nature of the segmented leg, different combinations of joint kinematics can lead to the same effective leg length and angle before TD, but to differing leg responses later during stance. Thus, we can expect that their combined analysis helps to infer quail motor control goals on rough terrains.

	Step up			Step down			Level
	1 cm	2.5 cm	5 cm	1 cm	2.5 cm	5 cm	
Speed (m s^{-1})	0.65 ± 0.12	0.55 ± 0.2	0.56 ± 0.2	**0.86 ± 0.3** (**)	0.51 ± 0.24	**0.44 ± 0.17** (*)	0.6 ± 0.11
Contact time (s)							
Trailing	0.23 ± 0.03	0.30 ± 0.12	0.24 ± 0.06	0.22 ± 0.1	**0.29 ± 0.1** (*)	**0.33 ± 0.09** (*)	0.22 ± 0.05
Leading	0.22 ± 0.03	0.33 ± 0.19	**0.28 ± 0.06** (*)	0.17 ± 0.06	0.21 ± 0.06	0.21 ± 0.06	
Swing time (s)							
Trailing	**0.17 ± 0.1** (*)	**0.23 ± 0.12** (*)	**0.20 ± 0.03** (*)	0.14 ± 0.01	0.19 ± 0.03	0.14 ± 0.03	0.14 ± 0.04
Leading	**0.17 ± 0.1** (**)	**0.22 ± 0.1** (*)	0.17 ± 0.04	**0.17 ± 0.01** (***)	**0.20 ± 0.02** (****)	**0.20 ± 0.05** (*)	

Table 1. Spatiotemporal parameters. Bold marked mean values indicate significant differences related to level locomotion. Significance codes: '****' ($p < 0.0001$); '***' ($p < 0.001$); '**' ($p < 0.01$); '*' ($p < 0.05$).

In this study, we aimed to uncover pelvic, leg, and joint kinematic adaptations to visible steps (upwards and downwards, Fig. 1), and how these adaptations influence leg response after TD. We searched for relationships between simple model representations of the leg and joint kinematics.

In our experiments, we used biplanar fluoroscopy to accurately describe joint positions in three dimensions (Fig. 1A,B). Because of our constrained field of view, we focused our analysis on preadaptation strategies, i.e., from the stride before the vertical shift in terrain (we termed i-1) to stride after that (termed i).

We expected step-type (up vs. down) and step-height related changes in leg kinematics, as animals preadapt and redirect the body when negotiating a visible vertical step. While kinematics cannot predict dynamics, we anticipated that the knowledge of the interaction between kinematics and dynamics during level locomotion discussed previously[3,4,14,15,18,21,22,24,38] could help us to deduce joint related pre-/post-adaptations and thus to infer the main goals of neuromechanical strategies used by animals to cope with vertical steps.

Results

Quails negotiated vertical steps ranging from ca. 10–50% of their effective leg length without major problems. None of the subjects lost visible stability or stumbled because of the challenges. Furthermore, based on the inspection of the live videos, they looked recovered from vertical shifts after one or two steps. To overcome 1 cm vertical steps, quails usually switched to aerial running for both step-up and step-down conditions. For negotiating 2.5 cm and 5 cm steps, quails relied on double support phases, except for 5 cm drops, where they sometimes switched to aerial running after the vertical shift. On average, locomotion speed measured during coping with the uneven substrate decreased with step height (Table 1). Contact and swing times showed a less clear trend. During step-up experiments, quails increased contact and swing times from 1 to 2.5 cm but decreased them from 2.5 to 5 cm step heights. For 2.5 cm and 5 cm, contact times were longer for the leading leg, indicating a reduction in the kinetic energy after the vertical shift. During step-down locomotion, the quail increased trailing limb contact times with step height, and varied swing times similarly as already explained for the step-up locomotion. For the leading, limb contact and swing times increased while increasing step height from 1 to 2.5 cm, but they did not vary between 2.5 and 5 cm step height.

In the following only selected significant differences are presented, please refer to the tables for further information about significance values.

Analysis of effective leg kinematics. *Stepping up, trailing leg.* Overall patterns of the effective leg length for the trailing limb were similar for level and step-up locomotion. After TD, the effective trailing leg is compressed, then slightly extended until toe-off (TO). During the swing, the leg shortened and rapidly extended until the next TD. The extension is decelerated at late swing (see Fig. 2A). However, some differences can be observed between level and step-up locomotion. Quails prepare step-up TD with longer effective trailing legs than observed during level locomotion. During stance, step-up conditions caused increased trailing leg extension (e.g., $l = 0.094$ m at TO during level locomotion versus $l = 0.139$ m at TO for the 5 cm step-up condition) and reduced leg retraction significantly compared to level locomotion ($\alpha_{TO} \approx 108°$, $\alpha_{TO} \approx 89°$, $\alpha_{TO} \approx 96°$, and $\alpha_{TO} \approx 100°$ for level, 1 cm, 2.5 cm, 5 cm, respectively; see Fig. 2C; Table S1).

Stepping up, leading leg. In general, the effective kinematics of the leading leg during step-up locomotion were similar to those observed during level locomotion. However, the effective leg length at TD (l_0) was significantly longer during step-up locomotion as compared to level locomotion ($l_{0\text{-level}} \approx 0.13$ m, while $l_{0\text{–}1\ cm}$, $l_{0\text{–}2.5\ cm}$, and $l_{0\text{–}5\ cm} > 0.14$ m, for all cases $p < 0.0001$). The trajectory of the effective leg angle (α) on the step was not substantially altered as compared to level locomotion, but differences were observed (Fig. 2D). For example, the leading leg starts the swing phase more vertically oriented and contacts the elevated substrate with a slightly less vertical angle compared to level locomotion (at TD, $\alpha_0 \approx 43°$, $\alpha_0 \approx 38°$, $\alpha_0 \approx 39°$, and $\alpha_0 \approx 36°$ for level, 1 cm, 2.5 cm, 5 cm, respectively, in all cases $p < 0.0001$). Retraction speed at TD was found to be significantly slower for 1 cm and 2.5 cm step heights compared to level locomotion ($\alpha_{0\text{-level}} \approx 300°\ s^{-1}$, $\alpha_{0\text{–}1\ cm} \approx 256°\ s^{-1}$, $\alpha_{0\text{–}2.5\ cm} \approx 235°\ s^{-1}$, $p < 0.012$ and $p < 0.001$, respectively, see Table S1b). Like the trailing leg, the leading leg was significantly ($p < 0.0001$) less retracted during stance compared to level locomotion ($\alpha_{85\%} \approx 89°$, $\alpha_{85\%} \approx 86°$, $\alpha_{85\%} \approx 86°$, and $\alpha_{85\%} \approx 85°$ for

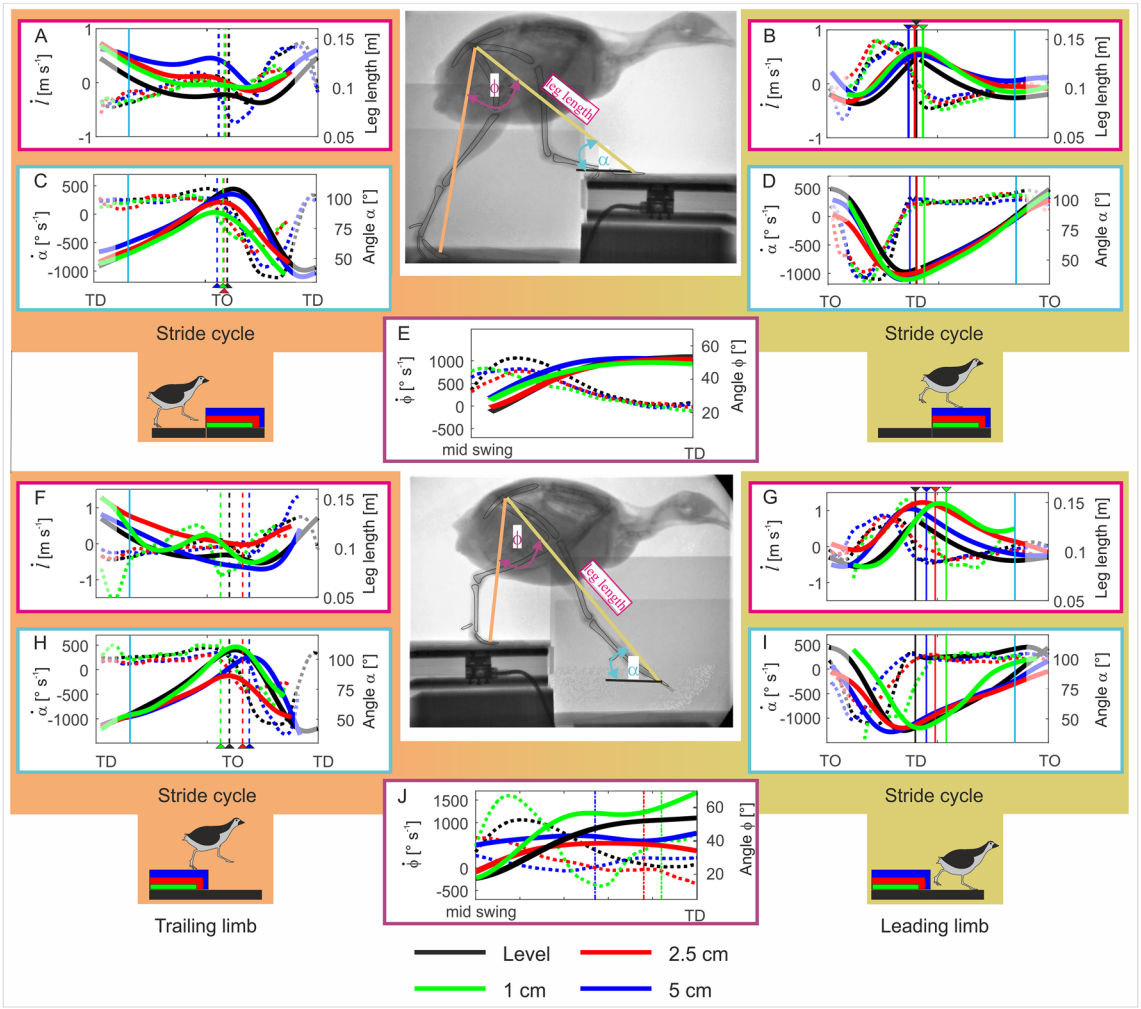

Figure 2. Effective leg kinematics during level and step locomotion. Level vs step-up (above): (**A**,**B**) effective leg length (l), effective leg axial velocity ($\dot{l}$). (**C**,**D**) effective leg angle (α), effective leg angle velocity ($\dot{\alpha}$). (**E**) aperture angle between effective legs (ϕ) and aperture angle velocity ($\dot{\phi}$). Level vs drop (below): (**F**,**G**) effective leg length (l), effective leg axial velocity ($\dot{l}$). (**H**,**I**) effective leg angle (α), effective leg angle velocity ($\dot{\alpha}$). (**J**) aperture angle between effective legs (ϕ) and aperture angle velocity ($\dot{\phi}$). Left: trailing leg stepping before the step up/downwards (stride i-1), right: leading leg stepping after the step up/downwards (stride i). Level (black) and step locomotion (1 cm: green, 2.5 cm: red, 5 cm: blue) in the quail. Solid lines: length/angle, dotted lines length/angle velocities. Curves display mean values. Black, blue, red, green dashed lines indicate toe-off (TO), while solid lines touch down (TD). Cyan solid lines indicate 15% and 85% of the stride. Due to the constrained field of view in the X-ray fluoroscope, hip data was often missing at the beginning and at the end of the stride cycles and average values less reliable (showed diffuse).

level, 1 cm, 2.5 cm, 5 cm, respectively). Differences between different steps heights were not significant (Fig. 2D; Table S2).

The aperture angle between leading and trailing legs at TD (ϕ_0) was generally not affected by step height and remained not significantly different from the mean values ($\phi_0 \approx 53°$) obtained during level locomotion (p value > 0.05, see Fig. 2E; Table S1).

Stepping down, trailing leg. Step related strategies were observed for the trailing leg at the level of the effective leg. Birds negotiating 1 cm drops displayed a compression-extension pattern that diverged from the pattern they exerted during level locomotion and from the monotonic compression displayed when they faced 2.5 cm and 5 cm steps (Fig. 2F). Stance time was significantly increased ($p < 0.05$) for drop heights of ca. 25% and 50% of leg length (level ≈ 0.22 s, 1 cm ≈ 0.22 s, 2.5 cm ≈ 0.29 s, 5 cm ≈ 0.33 s). Leg compression was significantly larger at TO for 5 cm drops ($p < 0.0001$) when compared to level locomotion and the other drop conditions ($l_{5cm} \approx 0.08$ m vs. $l_{2.5\ cm} \approx 0.107$ m, $l_{1cm} \approx 0.104$ m, $l_{level} \approx 0.094$ m).

The trailing leg's angle at the early stance (α) was not related to the height of the step-down, and it was similar to the α_0 observed for level locomotion ($\alpha_{15\%} \approx 54°$, see Fig. 2H; Table S1). For moderate drop heights, the effective leg angle was substantially ($p < 0.0001$) less retracted at TO ($\alpha_{TO} \approx 108°$, $\alpha_{TO} \approx 104°$, $\alpha_{TO} \approx 83°$, and $\alpha_{TO} \approx 106°$

for level, 1 cm, 2.5 cm, 5 cm, respectively; see Fig. 2H, Table S2). After TO the effective leg angle returned to the values observed during level locomotion.

Stepping down, leading leg. There were clear adaptations in effective leg kinematics for the leg that stepped on the lowered substrate. The effective leg length at TD for 5 cm steps ($l_{5cm} \approx 0.14$ m) was significantly shorter than the leg length at TD for 1 cm ($l_{5cm} \approx 0.15$ m) and 2.5 cm ($l_{5cm} \approx 0.15$ m) drops (in both cases p value < 0.0001, see Table S1). However, all three were significantly longer (p value < 0.0001) than the leg length observed during level locomotion $l_{level} \approx 0.13$ m. Leg compression speed at TD was also higher for the largest drops but not significantly different among step conditions (Fig. 2G, Table S1b). During stance, the effective leg was compressed until TO. However, at 85% of the stance, for all drops conditions, the effective leg length was significantly larger (p value < 0.0001) than the leg length measured during level locomotion ($l_{85\%} \approx 0.091$ m, $l_{85\%} \approx 0.122$ m, $l_{85\%} \approx 0.11$, and $l_{85\%} \approx 0.097$ for level, 1 cm, 2.5 cm, 5 cm, respectively).

Similarly, effective leg angles were altered during step down locomotion for the leading leg. At TO (elevated substrate) the angle of the effective leg stepping onto the lowered subtract was steeper as compared to level locomotion (level $\alpha_{TO} \approx 108°$, from Table S2, 2.5 cm: $\alpha_{TO} \approx 89°$, 5 cm: $\alpha_{TO} \approx 87°$, from Fig. 2I). At TD, the angle of attack (α_0) was unrelated to drop-height but significantly more retracted after a drop compared to level locomotion ($\alpha_{0\text{-level}} \approx 42°$, $\alpha_{0\text{-1 cm}} \approx 50°$, $\alpha_{0\text{-2.5 cm}} \approx 54°$, and $\alpha_{0\text{-5 cm}} \approx 53°$, in all cases p value < 0.001; see Table S1). Retraction speed at TD ($\dot{\alpha}_0$) was significantly reduced for drops of 25% and 50% of leg length ($\dot{\alpha}_{0\text{-level}} \approx 300° \text{ s}^{-1}$, $\dot{\alpha}_{0\text{-2.5 cm}} \approx 243° \text{ s}^{-1}$, $\dot{\alpha}_{0\text{-5 cm}} \approx 200° \text{ s}^{-1}$; $p < 0.01$ and $p < 0.0001$, respectively).

The aperture angle (ϕ_0) between leading and trailing legs was adapted to the drop height (Fig. 2J). For 1 cm step, the aperture angle increased before TD especially after the level height was crossed. Conversely, for 2.5 cm and 5 cm drops, the aperture angle was on average significantly below the mean value obtained at level locomotion ($\phi_{0\text{-level}} \approx 53°$, $\phi_{0\text{-2.5 cm}} \approx 35°$, $\phi_{0\text{-5 cm}} \approx 44°$, and $\phi_0 \approx 53°$, p value < 0.0001, respectively p value < 0.01; Table S1). Note that the quails adapted the angle between legs after the point at which level height was crossed (Fig. 2J).

Joint angles. The previous section described how effective leg kinematics were altered during uneven locomotion. In this section, we describe how the kinematics of individual, elemental joints were altered. Quail joint angles during level locomotion were previously published[3]. Here, we have included pertinent values from that study to permit the comparison between step and level locomotion. The influence of the disturbances on the hip angle will be described in the section on 3D hip angles.

Stepping up, trailing limb (Fig. 3A,C,E). To negotiate 1 cm steps, quails used significantly more flexed knee (Fig. 3A) and INT angles (Fig. 3C) in the early stance as compared to level locomotion (around 15% stance: $knee_{1cm} \approx 85°$ vs. $knee_{level} \approx 98°$, $p < 0.0001$; $INT_{1cm} \approx 99°$, $INT_{level} \approx 112°$). Around TO the knee was more extended while the INT remained more flexed compared to level locomotion ($knee_{1cm} \approx 64°$ vs. $knee_{level} \approx 60°$, $p = 0.04$; $INT_{1cm} \approx 81°$, $INT_{level} \approx 112°$, $p < 0.0001$). 2.5 cm steps induced less substantial but still significant changes in knee and TMP joint kinematics (Fig. 3E). Both the knee and the TMP were more flexed in the early stance (around 15% stance: $knee_{2.5\ cm} \approx 91°$ vs. $knee_{level} \approx 98°$, $p < 0.0001$; $TMP_{2.5\ cm} \approx 135°$ vs $TMP_{level} \approx 143°$, $p < 0.01$). The knee was around TO significantly more expended (around TO: $knee_{2.5\ cm} \approx 73°$ vs. $knee_{level} \approx 60°$, $p < 0.0001$). To negotiate 5 cm steps, the knee and the INT joints were significantly more extended, and the TMP was more flexed during early stance. Around 15% stance: $knee_{5cm} \approx 113°$ vs. $knee_{level} \approx 98°$, $p < 0.0001$; $INT_{5cm} \approx 139°$, $INT_{level} \approx 112°$, $p < 0.0001$; $TMP_{5cm} \approx 135°$ vs $TMP_{level} \approx 143°$, $p < 0.01$. Around TO: $knee_{5cm} \approx 103°$ vs. $knee_{level} \approx 60°$, $p < 0.0001$; $INT_{5cm} \approx 143°$, $INT_{level} \approx 112°$, $p < 0.0001$; $TMP_{5cm} \approx 142°$, $TMP_{level} \approx 142°$, $p > 0.05$ (see Fig. 3A,C,E, Tables S3, S4).

After TO, the knee was kept more extended during the early swing phase. Note that the bouncing behavior observed in the INT almost vanishes when facing 5 cm step upwards (Fig. 3C).

Stepping up, leading limb (Fig. 3B,D,F). In the elevated substrate, the quails displayed in average a more flexed knee and INT at TD for all experimental conditions (Fig. 3B,D, $knee_{level} \approx 120°$, $knee_{1cm} \approx 106°$, $knee_{2.5\ cm} \approx 112°$, $knee_{5cm} \approx 110°$, all $p < 0.0001$; $INT_{level} \approx 125°$, $INT_{1cm} \approx 112°$,$INT_{2.5\ cm} \approx 114°$, $INT_{5cm} \approx 121°$, for 1 cm and 2.5 cm $p < 0.0001$, for 5 cm $p = 0.058$, see Table S3). During stance on the step, the joint patterns for 1 cm and 2.5 cm steps displayed a more flexed INT (Fig. 3D), together with a more extended TMP (Fig. 3F) compared to the patterns observed for 5 cm steps.

Stepping down, trailing limb (Fig. 3G,I,K). When negotiating 1 cm steps, the flexion–extension pattern for the TMP changed (Fig. 3K). Note that during stance, there was a larger flexion up to midstance, followed by an extension in the late stance. After TO, a second more marked flexion extension was exhibited. For 2.5 cm drops, quails displayed less flexion extension in the INT Fig(3I). More marked differences in all joints were observed for 5 cm steps. Under this test condition, knee (Fig. 3G) and INT joints exhibited significantly larger flexion at TD and during stance. Around 15% stance: $knee_{5cm} \approx 90°$ vs. $knee_{level} \approx 98°$; $INT_{5cm} \approx 76°$, $INT_{level} \approx 112°$, both $p < 0.0001$. Around TO: $knee_{5cm} \approx 48°$ vs. $knee_{level} \approx 60°$; $INT_{5cm} \approx 81°$, $INT_{level} \approx 112°$, both $p < 0.0001$). After TO, knee and INT were kept more flexed (see Fig. 3G,I).

Stepping down, leading limb (Fig. 3H,J,L). The leg that stepped in the lowered substrate, displayed step related adaptations before and after TD. Before TD, changes were observed mainly in the distal joints. 1 cm drops increased joint flexion in the first half of the swing phase but did not induce significant changes at TD related to level locomotion. 2.5 cm and 5 cm drops did not substantially influence joint swing patterns but affected joint

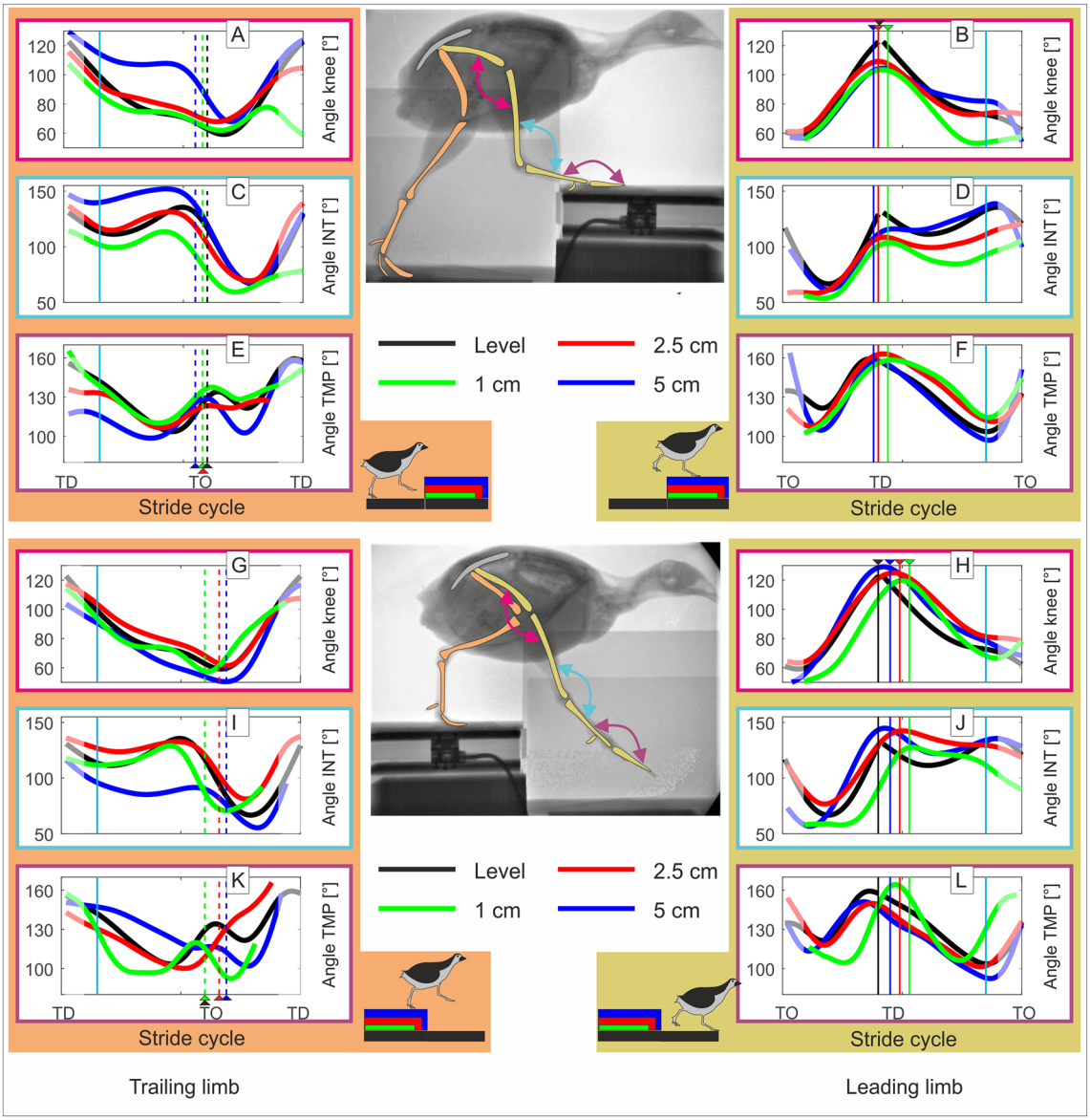

Figure 3. Joint angles. Level vs step-up (above): (**A**,**B**) knee; (**C**,**D**) intertarsal (INT); and (**E**,**F**) tarsometatarsal-phalangeal (TMP). Level vs drop (below): (**G**,**H**) knee; (**I**,**J**) INT; and (**K**,**L**) TMP. Left: trailing leg stepping before the step up/downwards (stride i-1), right: leading leg stepping after the step up/downwards (stride i). Curves display mean values of joint angles during level (black) and step locomotion (1 cm: green, 2.5 cm: red, 5 cm: blue) in the quail. Black, blue, red, green dashed lines indicate toe-off (TO), while solid lines touch down (TD). Cyan solid lines indicate 15% and 85% of the stride. Due to the constrained field of view in the X-ray fluoroscope, hip data was often missing at the beginning and at the end of the stride cycles and average values might be less reliable (showed diffuse).

angles at TD (related to level locomotion, significantly more extended for the knee and INT: $knee_{level} \approx 120°$, $knee_{2.5\ cm} \approx 128°$, $knee_{5cm} \approx 131°$, both $p < 0.0001$; $INT_{level} \approx 125°$, $INT_{2.5\ cm} \approx 146°$, $INT_{5cm} \approx 148°$, both $p < 0.0001$, see Fig. 3H,J, Table S3, and significantly more flexed for the TMP: $TMP_{level} \approx 158°$, $TMP_{2.5\ cm} \approx 133°$, $TMP_{5cm} \approx 134°$, both $p < 0.0001$, see Fig. 3L and Table S3). After TD, the INT was further flexed for 1 cm and 2.5 cm drops until TO (Fig. 3J). The INT for 5 cm and the TMP for 1 cm drops displayed a rebound behavior (flexion–extension pattern, see Fig. 3J). For 2.5 cm and 5 cm drops, TMP patterns were like those observed for level locomotion, but the joints were kept more flexed until late stance (Fig. 3L).

3D-kinematics of the whole leg. This section describes the three-dimensional kinematics of the whole leg relative to the pelvis during level and step locomotion (see Fig. 4). Under the assumption that both knee and intertarsal joints work as revolute joints, the whole leg approximates three-dimensional hip kinematics. Note that because the z-axis was aligned with the segment from hip to knee, rotation about y-axis (β_h) reflects flexion/extension between femur and pelvis, rotations about z-axis (γ_h) reflect hip ab-adduction, while rota-

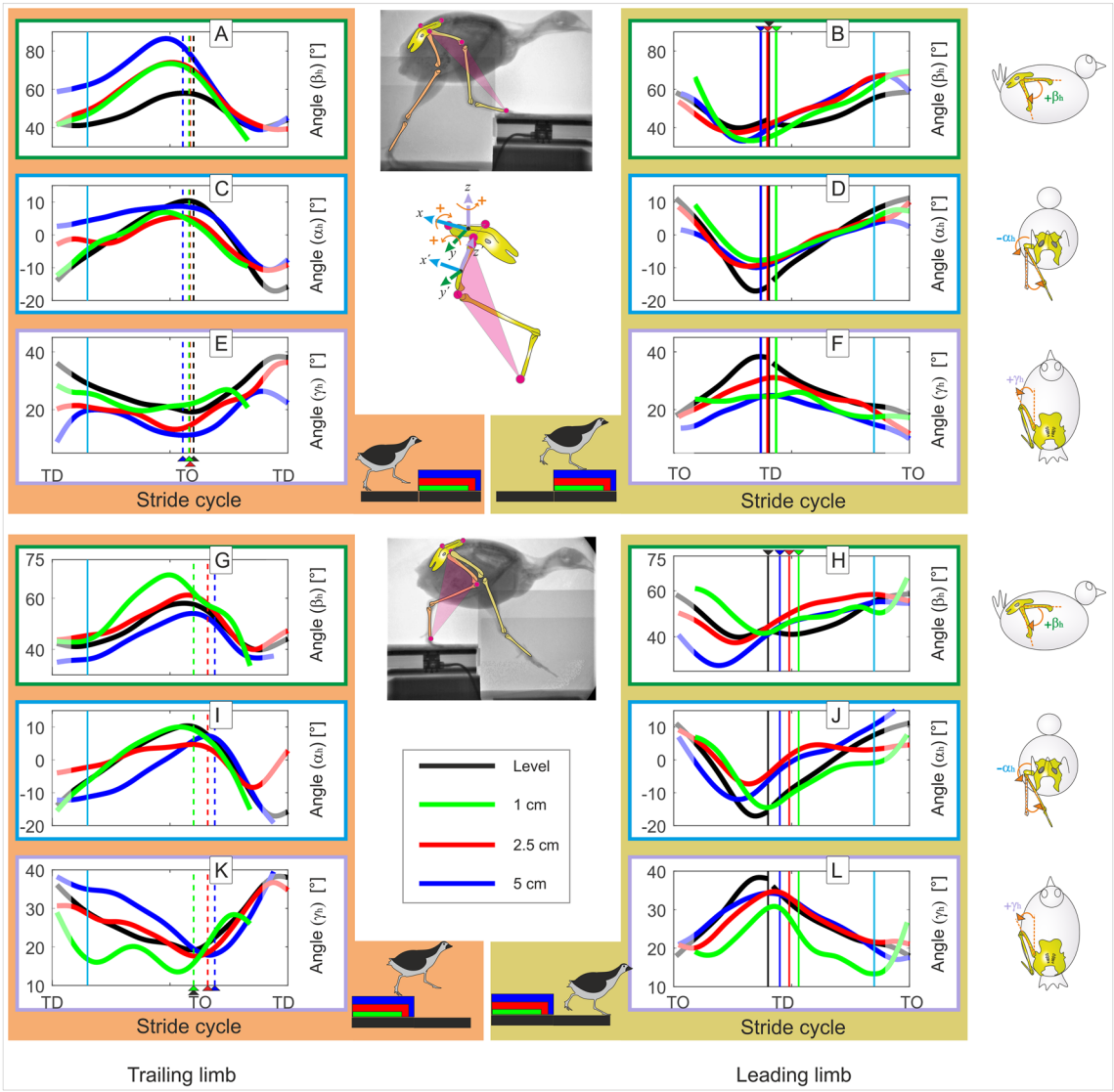

Figure 4. Whole leg three-dimensional rotations in the quail. Motions were measured relative to the pelvis. Level (black) and step locomotion (1 cm: green, 2.5 cm: red, 5 cm: blue). Accepting that the knee, the intertarsal and the tarsometatarsal–phalangeal joints work mainly as revolute joints, the plane describing the whole-leg displays the three-dimensional hip control. Level vs step-up (above): (**A**,**B**) hip flexion extension (β_h), negative values indicate flexion. (**C**,**D**) Hip mediolateral rotation (α_h). Positive values indicate that the distal point of the whole leg moves laterally with respect to the hip; and (**E**,**F**) hip ad-abduction (γ_h). Level vs drop (below): (**G**,**H**) hip flexion extension; (**I**,**J**) mediolateral rotation; and (**E**,**F**) hip Ad-abduction. Curves display mean values. Left: trailing leg stepping before the step up/downwards (stride i-1), right: leading leg stepping after the step up/downwards (stride i). Black, blue, red, green dashed lines indicate toe-off (TO), while solid lines touch down (TD). Cyan solid lines indicate 15% and 85% of the stride. Due to the constrained field of view in the X-ray fluoroscope, hip data was often missing at the beginning and at the end of the stride cycles and average values might be less reliable (showed diffuse).

tions about the x-axis (α_h) reflect femoral axial rotations, resulting in the mediolateral rotation of the whole leg. $\alpha_h = \beta_h = \gamma_h = 0°$ indicates that the whole leg and the pelvis coordinate systems are aligned. However, in this zero-pose, the pelvis and femur are orthogonal to each in the sagittal plane. Therefore, we used $\beta_h + 90°$ to represent hip flexion/extension in Fig. 4A,B,G,H and Tables S5 and S6. In the following, level locomotion is first described in detail. Step locomotion is discussed when there is a difference from level locomotion.

Level locomotion, hip flexion–extension (β_h). At TD, the hip joint is flexed about 42°. After a small flexion due to weight transfer, the hip joint extends 17° until TO. After TO the leg protracts, flexing the hip joint up to 85% of swing. In the late swing phase, the whole leg retracts until TD (see Fig. 4A, black line).

Level locomotion, mediolateral control of the whole leg (α_h). At TD the whole leg was medially oriented ($\alpha \approx -14°$). During stance, the leg was rotated laterally until TO to an angle of approx. $\alpha = 11°$. During swing, the distal point of the whole leg was rapidly rotated medially (see Fig. 4C, black line).

Level locomotion, whole leg (femoral) ab-adduction (γ_h). Hip ab-adduction curves show a half-sine pattern. At TD the whole leg was abducted about 36°. Abduction was reduced during stance to 18° at TO. After TO the leg was abducted up to TD (see Fig. 4E, black line).

Stepping up, trailing limb (Fig. 4,A,C,E; Tables S5,S6). Step height had a significant influence on hip flexion–extension. At TD, quails facing step-ups exhibited significant larger hip extension (Fig. 4A). As stance phase progressed, the hip joint was significantly more extended during stepping up than during level locomotion (around 15% stance: $\beta_{\text{h-level}} \approx 41°$, $\beta_{\text{h-1 cm}} \approx 46°$, $\beta_{\text{h-2.5 cm}} \approx 49°$, $\beta_{\text{h-5 cm}} \approx 62°$, p values = 0.0042, 0.00003, and 0 for 1 cm, 2.5 cm, and 5 cm, respectively). However, 1 cm and 2.5 cm steps induced, on average, similar hip extension patterns (p value > 0.05) but significantly different from 5 cm (i.e., quails displayed a two-step strategy to negotiate the different step-up conditions). Mediolateral hip control was also influenced by step height (Fig. 4C). At TD and early stance, 2.5 cm and 5 cm step-ups induced a more vertical orientation of the whole leg (around 15% stance: $\alpha_{\text{h-level}} \approx -6°$, $\alpha_{\text{h-1 cm}} \approx -4°$, $\alpha_{\text{h-2.5 cm}} \approx -2°$, $\alpha_{\text{h-5 cm}} \approx 6°$, p values < 0.0001 for 2.5 cm, and 5 cm), and at TO the whole leg was less laterally oriented than during level locomotion (around TO: $\alpha_{\text{h-level}} \approx 11°$, $\alpha_{\text{h-1 cm}} \approx 5°$, $\alpha_{\text{h-2.5 cm}} \approx 5°$, $\alpha_{\text{h-5 cm}} \approx 9°$, p values < 0.0001 for 1 cm, and 2.5 cm). During step-up locomotion, the whole leg was on average less abducted (Fig. 4E). While quails facing 5 cm steps decreased abduction in similar way as when they negotiated 2.5 cm steps, for coping with 1 cm steps they kept adduction similar to the abduction observed during level locomotion (around 15% stance: $\gamma_{\text{h-level}} \approx 29°$, $\gamma_{\text{h-1 cm}} \approx 27°$, $\gamma_{\text{h-2.5 cm}} \approx 21°$, $\gamma_{\text{h-5 cm}} \approx 20°$, p values < 0.0001 for 2.5 cm, and 5 cm; around TO: $\gamma_{\text{h-level}} \approx 18°$, $\gamma_{\text{h-1 cm}} \approx 22°$, $\gamma_{\text{h-2.5 cm}} \approx 14°$, $\gamma_{\text{h-5 cm}} \approx 10°$, p values < 0.0001 for 2.5 cm, and 5 cm). After TO, quails facing 2.5 cm and 5 cm steps increased abduction, approaching values observed during level locomotion. However, for 5 cm steps, quails maintained a persistent hip adduction in the late swing.

Stepping up, leading limb (Fig. 4B,D,F and Tables S5 and S6). Flexion–extension patterns in the elevated step are similar in shape to those observed for level locomotion (Fig. 4B). However, the quail stepped with a more flexed hip after negotiating 1 cm and 5 cm steps (around TD: $\beta_{\text{h-level}} \approx 42°$, $\beta_{\text{h-1 cm}} \approx 37°$, $\beta_{\text{h-2.5 cm}} \approx 42°$, $\beta_{\text{h-5 cm}} \approx 38°$, p values < 0.0001 for 1 cm and 5 cm). After TD, the quail exhibited comparative larger hip extensions compared to level locomotion (at late stance, around 85%: $\beta_{\text{h-level}} \approx 56°$, $\beta_{\text{h-1 cm}} \approx 62°$, $\beta_{\text{h-2.5 cm}} \approx 68°$, $\beta_{\text{h-5 cm}} \approx 66°$, p values < 0.0001 for 1 cm, 2.5 cm and 5 cm). In contrast, the quail reduced both mediolateral rotations (Fig. 4D) and ab-adduction (Fig. 4F) during the swing phase before stepping on the elevated substrate. At TD on the elevated substrate, the leading whole leg was significantly more vertically oriented and less abducted compared to level locomotion (around TD: $\alpha_{\text{h-level}} \approx -15°$, $\alpha_{\text{h-1 cm}} \approx -7°$, $\alpha_{\text{h-2.5 cm}} \approx -8°$, $\alpha_{\text{h-5 cm}} \approx -9°$, for all cases p value < 0.0001; $\gamma_{\text{h-level}} \approx 37°$, $\gamma_{\text{h-1 cm}} \approx 25°$, $\gamma_{\text{h-2.5 cm}} \approx 30°$, $\gamma_{\text{h-5 cm}} \approx 25°$, all p values < 0.0001). After the early stance phase, mediolateral motion differences between step and level locomotion lessened (around 85% stance: $\alpha_{\text{h-level}} \approx 8°$, $\alpha_{\text{h-1 cm}} \approx 5°$, $\alpha_{\text{h-2.5 cm}} \approx 5°$, $\alpha_{\text{h-5 cm}} \approx 3°$, p value < 0.0001 for 5 cm). For 1 cm steps, the abduction of the whole leg stayed around $\gamma = 20°$ (Fig. 4F).

Stepping down, trailing limb (Fig. 4G,I,K, and Tables S5 and S6).. Quails facing 1 cm visible drops displayed larger hip extension after midstance (Fig. 4G). This can be explained by the tendency of the subjects to switch to aerial running when negotiating this type of step height. 2.5 cm drops did not induce major changes in the flexion–extension patterns of the hip. When negotiating 5 cm drops, the hip joint was significantly more flexed than during level locomotion (around 15% stance: $\beta_{\text{h-level}} \approx 41°$, $\beta_{\text{h-5 cm}} \approx 36°$, p value < 0.0001; around TO: $\beta_{\text{h-level}} \approx 57°$, $\beta_{\text{h-5 cm}} \approx 52°$, p value < 0.001).

The response of the mediolateral hip control for 1 cm and 2.5 cm was similar to those observed during step upwards Fig. (4I). For 5 cm drops, the leg was more medially oriented at TD than observed during level locomotion (around 15% stance: $\alpha_{\text{h-level}} \approx -6°$, $\alpha_{\text{h-5 cm}} \approx -11°$, p < 0.0001) and straightening of the leg during stance was more gradual.

The abduction of the leg (Fig. 4K) increased with drop height (p < 0.001). When quails faced 1 cm steps, adduction of the whole leg was reduced with respect to level locomotion. When they negotiated 2.5 cm steps, abduction was on average similar to the patterns exhibited during level locomotion, while for 5 cm drops, the whole leg was kept more abducted until late stance (around 15% stance: $\gamma_{\text{h-level}} \approx 29°$, $\gamma_{\text{h-1 cm}} \approx 16°$, $\gamma_{\text{h-2.5 cm}} \approx 28°$, $\gamma_{\text{h-5 cm}} \approx 34°$, p values < 0.0001 for 1 cm and 5 cm; around TO: $\gamma_{\text{h-level}} \approx 18°$, $\gamma_{\text{h-1 cm}} \approx 14°$, $\gamma_{\text{h-2.5 cm}} \approx 17°$, $\gamma_{\text{h-5 cm}} \approx 16°$, p < 0.0001 for 1 cm, and p = 0.02 for 5 cm).

Stepping down, leading limb (Fig. 4H,J,L, and Tables S5 and S6). Quails started the swing phase using a more extended hip to approach 1 cm drops, and more flexed for 2.5 cm and 5 cm drops (see Fig. 4H). At TD in the lowered substrate, the hip was more extended for 1 cm, 2.5 cm and 5 cm (around TD: $\beta_{\text{h-level}} \approx 42°$, $\beta_{\text{h-1 cm}} \approx 44°$, $\beta_{\text{h-2.5 cm}} \approx 52°$, $\beta_{\text{h-5 cm}} \approx 47°$, p values < 0.0001 for 2.5 cm and 5 cm).

Whole leg medial rotations (femoral outer rotations, Fig. 4J) were constrained when negotiating 2.5 cm and 5 cm drops (around TD: $\alpha_{\text{h-level}} \approx -15°$, $\alpha_{\text{h-2.5 cm}} \approx 3°$, $\alpha_{5\ \text{cm}} \approx -1°$, in both cases p < 0.0001). This permitted the quail to step in the lowered substrate with an almost vertically oriented whole leg.

Hip adduction was also reduced during the swing phase (Fig. 4L). After 1 cm drop, the quail kept their hip more adducted during stance (around TD: $\gamma_{\text{h-level}} \approx 37°$, $\gamma_{\text{h-1 cm}} \approx 23°$, p < 0.0001), but close before TO, the hip joint was abducted. After 2.5 cm and 5 cm drops, hip adduction behaved like the patterns observed for level locomotion (around TD: $\gamma_{\text{h-2.5 cm}} \approx \gamma_{\text{h-5 cm}} \approx 34°$, p > 0.05).

Pelvis. Because in Aves the pelvis and the trunk are fused[39], the three-dimensional kinematics of the pelvis informs about the spatial motion of the trunk as well. Pelvic pitch (βp) oscillation frequency was twice the step frequency, across all locomotion conditions compared to level locomotion, pelvic retroversion increased significantly ($p < 0.0001$) when the quail negotiated step up conditions: the pelvis was retroverted about 10° during level and up to 28° during step up locomotion (Fig. 5A). For visible drops, the picture was less clear and was inconsistent across different size drops (Fig. 5D). Relative to the values obtained for level locomotion, when quails faced 1 cm drops, they increased and then decreased pelvic retroversion after the TD in the lowered substrate. When they faced 2.5 cm drops, they significantly increased pelvic retroversion (mean values oscillated about $\beta_{p\text{-}2.5\ cm} \approx -20°$, with a p value < 0.001 in all three measured timepoints), and when quails negotiated 5 cm drops, they significantly decreased pelvic retroversion related to level locomotion (mean values were: at 15% stride, $\beta_{p\text{-}5\ cm} \approx -6°$, $p < 0.05$, at TD leading limb $\beta_{p\text{-}5\ cm} \approx -9°$, $p < 0.01$, at TO trailing limb $\beta_{p\text{-}5\ cm} \approx -7°$, $p < 0.0001$). For more information see Table S7.

Lateral tilt (α_p, roll) was cyclic and counteracted by the leg in contact with the substrate (Fig. 5B,E). Step-related differences were found for 2.5 cm and 5 cm after mid-stride ($p < 0.0001$) for both steps upwards and downwards. Relative to level locomotion, significant differences existed only for 5 cm upwards around the double support phase ($p < 0.01$, see Fig. 5B and Table S8). Pelvic yaw amplitudes (γ_p) were small. While during level locomotion, γ_p oscillated around cero. When negotiating the highest step-up condition, the quail rotated the pelvis towards the contralateral leg during the trailing support phase. This change was significant ($p < 0.001$, see Fig. 5C; Table S9). For drops of about 25% and 50% of leg length the quail rotated the pelvis about $\gamma_p \approx 8°$towards the direction of the leg in contact with the ground. Compared to level locomotion, those changes were significant ($p < 0.001$). To facilitate negotiating larger visible drops, the pelvis (and the trunk) were rotated towards the trailing limb (yaw) and tilted (roll) towards the leading leg. After TD in the lowered substrate, the pelvis (trunk) was reoriented in motion's direction.

Discussion

To understand control strategies implemented by any system, it is necessary to characterize how the system responds to external perturbations. In the present work, we analyzed the kinematic strategies employed by the common quail to negotiate visible step-up and step-down conditions of about 10%, 25%, and 50% of the average value of their effective leg length during stance. Our main goal was to uncover leg kinematic changes at different levels of abstraction and how they relate to each other. The highest level of abstraction in our work is found in the effective leg (Fig. 1F). The kinematic analysis of the effective leg characterizes global control goals such as leg length, angle of attack at TD, aperture angle and retraction speed. Note that the effective leg will have two main functions if the dynamics are taken into consideration: (a) the axial leg function, which is a time-dependent force function (e.g., spring-damper) and (b) the tangential or rotational leg function, which is a time-dependent torque that controls the leg and balances the trunk (e.g., virtual pivot point (VPP) control[22,40]). Two- and three-dimensional joint kinematics (Fig. 1E,D) are representations with less level of abstraction. Because different combinations of joint kinematics can lead to the same effective leg lengths, we expected that their combined analysis would help to infer quail motor control goals on uneven terrains. Thus, we compared the (a) effective leg kinematic, (b) joint kinematics and (c) whole leg (represents hip 3D kinematics, see Fig. 4) and pelvic kinematics for the quail negotiating step-up and step-down conditions with our previously collected data on quail level ground running[22], which is freely available on https://datadryad.org/stash/dataset/doi:10.5061/dryad.jh5h4.

Our results display a complex picture of kinematic strategies before and after TD. In the next sections, we analyze that complex picture by linking our results with the existing knowledge about the interactions between kinematics, dynamics, and muscle activation during level/uneven locomotion. This combined analysis is used to unravel anticipatory and reactive strategies for the negotiation of uneven terrain, and to discuss whether those strategies may be governed by simple control goals.

Stepping up. *Trailing limb (stride i-1).* The trailing effective leg was significantly longer at TD for stepping up condition than observed during level grounded running. Moreover, the effective leg length significantly increased with step height. The angle of attack at TD was steeper as step height increased. The differences in effective leg length between level locomotion and step locomotion at TD might be explained by the fact that data for level and step locomotion belonged to different quail cohorts. Animals had similar age, but the quail facing steps were heavier. However, longer effective leg length at TD and steeper angle of attack at TD might also indicate a "pre-programmed" control strategy at the global level to negotiate upward steps perhaps producing a shift in the operating locomotion program towards "mixed gaits"[24], a periodic change between walking and grounded running steps that might permit birds to adjust their leg to vault towards the elevated substrate[14]. A more extended leg at TD also would agree with observations in running humans, which adapt their center of mass (CoM) height about 50% of step height in anticipation of stepping onto a visible step[41,42]. Note that because of neuromuscular delays, vertebrates preset muscle force before TD using posture dependent control[3,14,15,17,43]. During stance, the quail also fine-tuned leg length, and leg retraction of the trailing effective leg according to step height (see Fig. 2A,C). This adjustment indicates that visual perception of the upcoming obstacle induced anticipatory changes in leg loading during stance. One can hypothesize that the goal of this sensory driven adaptation was to adjust the trajectory of the CoM to reduce the necessity of compensation in the following step.

How was the effective trailing leg length adjusted at the joint level in the step before the vertical shift? Our results suggest that the quail used two distinct strategies, depending on the height of the step. For step heights up to 25% of effective leg length, the extension of the hip joint lengthened the leg, while knee and intertarsal joints displayed similar patterns to those observed during level locomotion. For the 5 cm step height (about 50% of effective leg length) both knee and intertarsal joints were extended, while the hip joint extended even more.

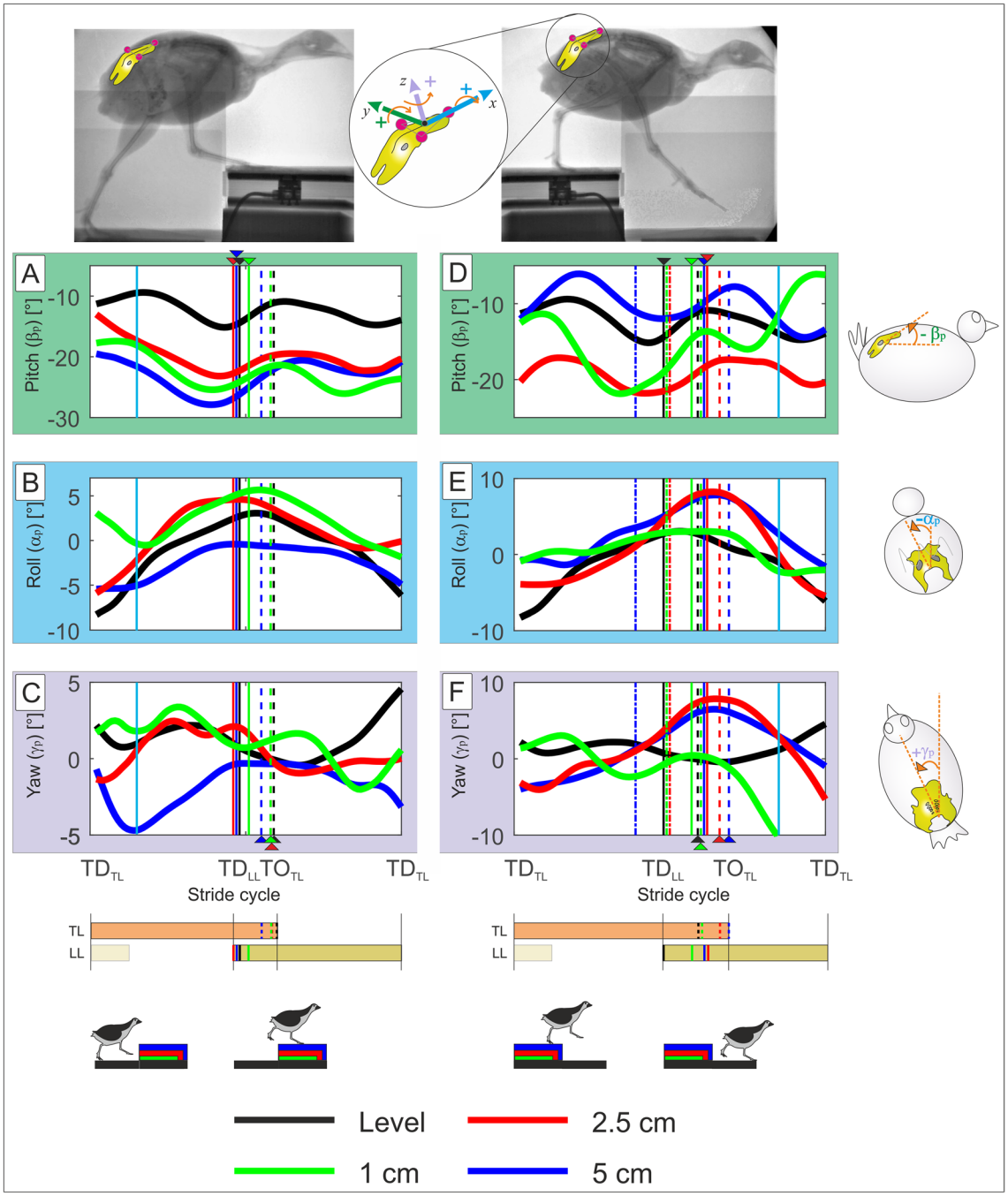

Figure 5. Pelvic three-dimensional rotations during level (black) and step locomotion in the quail. Curves display mean values. Left: step-up locomotion, right: step-down locomotion. For better understanding, we transformed the data to ensure that the trailing limb is always the left leg and the leading leg the right one (see methods). (**A**,**D**) pelvic pitch (β_p), negative values indicate retroversion (trunk is more vertical oriented). (**B**,**E**) pelvic roll (α_p), positive values indicate that the trunk tilts towards the right. (**C**,**F**) Pelvic yaw (γ_p), positive values indicate that the body is directed towards the left. Black, blue, red, green dashed lines indicate toe-off of the contralateral leg (TO), while solid lines touch down (TD). Dot dashed lines indicate when the leg crossed level line during drops. Cyan solid lines indicate 15% and 85% of the stride. *TL* trailing limb, *LL* leading limb. Due to the constrained field of view in the X-ray fluoroscope, hip data was often missing at the beginning and at the end of the stride cycles and average values might be less reliable.

Note that during quail level locomotion, the spring-like leg behavior is mostly produced in the INT, while the active flexion of the knee joint controls leg retraction[3,44]. However, to negotiate 5 cm steps, the extension of both knee and INT turned the crouched quail leg into a more vertical one. In this leg configuration, the retraction

of the leg is produced by hip extension. Thus, to vault the CoM onto the obstacle, the avian leg was controlled similarly as humans and animals, which have a more stiff and extended leg design[12,21,41,43,45–47].

Thus, the "zig-zag" configuration of the femur, the tibiotarsus, and the tarsometatarsus is abandoned to negotiate larger steps (see the trailing limb configuration superimposed to the X-ray picture in Fig. 3). The enclosed joints are spanned by mono- and bi-articular muscles with the latter enforcing a parallel mechanism, the so-called pantograph leg[48,49]. Gordon et al.[9] reported significant larger activations for muscles *M. flexor cruris lateralis pelvica* (FCLP, hip extensor, knee flexor, possible hip abductor), *M. gastrocnemius pars lateralis* (GL, ankle extensor, knee flexor), *M. gastrocnemius pars medialis* (GM, ankle extensor, knee flexor/extensor), *M. flexor perforatus digiti* III (FPPD3, ankle extensor, digital flexor), and *M. femorotibialis lateralis* (FTL, mono-articular knee extensor) in the step prior to a step-up condition. These activation profiles are consistent with the control of the extension in the hip joint, the knee and the INT in the quail. In addition, the larger activation of FCLP also correlates with the reduced hip adduction in the quail when negotiating 5 cm step upwards. At the neuronal level, this shift in leg behavior might be induced by changed muscle synergies via higher locomotor center signals based on visual perception.

Leading leg towards and on the elevated substrate (stride i). When the leading limb was swung towards the elevated substrate, the quail controlled the aperture angle between legs as described for level locomotion[4]. In the late swing, the aperture angle was kept constant at $\phi \approx 53°$ despite step height. Thus, the late swing retraction and the angle of attack of the leading leg were mainly controlled by the retraction of the trailing leg, as hypothesized.

When the leading leg stepped on the elevated substrate, the effective leg length and the angle of attack were similar to those observed in level locomotion. After TD, the effective leading leg kinematics did not markedly differ from those observed during level locomotion. Adaptations of the trailing limb thus permitted the leading limb to touch down on the step in similar manner as during level locomotion. This strategy might help to rapidly dissipate the changes in state variables produced by the vertical step. Empirical evidence has shown that running animals recover steady state behavior two to three steps after an unexpected perturbation[15,50,51]. Our observations from live videos suggest that the quail recovered from a visible step upwards or drop mostly in the second step after it, similarly, as described previously for other birds[9,14,15].

Despite the significant extension of the trailing leg, the leading leg touched down with joints more flexed than during level locomotion. After TD, the hip was rapidly more extended than during level locomotion, and the behavior of the INT shifted from a spring-like mode to an energy supplier (joint extended beyond its angle at TD) as step height increased. Note that at TD, the knee was not used to extend the leg, possibly because larger extensor torques about this joint would increase the horizontal GRF, breaking the retraction of the leg. Even so, the flexion of the knee was controlled during stance when negotiating the largest step heights, so that the knee-joint angle returned slowly to the value exhibited during unrestricted locomotion. The increased extensor activity of the FTL muscle, observed after the guinea fowl stepped on an elevated substrate, might be consistent with our observations[9].

In summary, the trailing leg extension might have reduced the necessity of reactive control. Whether changes in leading leg loading are necessary to compensate for the more flexed joints at TD, must be investigated in further studies.

Stepping down. *Trailing limb (stride i-1).* When the quail negotiated drops of about 10% of effective leg length, they used aerial phases to rapidly overcome the challenge. To introduce aerial phases, the operation of the trailing leg was shifted towards spring-like behavior (more marked rebound, see Fig. 2F). At the effective leg level, this change can be produced by reducing effective leg damping and/or inducing an axial extension of the effective leg in the late stance. In both cases, the pronograde virtual pivot point model [PVPP[22]] predicts that the axial energy of the system increases. This makes aerial phases more likely to occur. But how are those changes produced at the joint level? As observed before[3] and for step-up conditions, hip extension seems to control effective leg extension if legs are kept crouched (c.p. Figs. 2A, 4A). Knee and INT joint kinematics did not display sudden changes compared to level locomotion (Fig. 3G,I, green lines). This seems to indicate, following[3], that retraction angle was not adapted to negotiate the lowest drop height. Indeed, the trajectories for the retraction angle did not deviate from those observed during level locomotion (see Fig. 2H). As explained before, the INT seems to control the spring-like behavior of the avian leg[3]. Taking this into account, the shape of the curve in Fig. 3G might indicate that the spring-like behavior was conserved in the INT (note the rebound behavior compared to level locomotion). However, this hypothesis and the relationship between stiffness changes in the INT and their influence in the effective leg stiffness need further analysis.

When compared with the patterns obtained during level locomotion, the TMP joint displayed a change to a more spring-like function (see Fig. 3K). Because this joint was previously related to the damping behavior of the leg during level locomotion[3], we can speculate, based on the PVPP model, that the combined action of the hip and the TMP joints might control gait-changes between grounded and aerial running as they regulate, respectively, the effective leg length and damping ratio during the stance.

To cope with drops of about 25% to 50% of leg length, the quail approached the step slower compared to 1 cm and relied on double support. Animals' strategies to negotiate drops of 25% and 50% leg length differed. When negotiating visible drops of 25% leg length, the quail displayed rather subtle changes in the trailing leg, even though its effective length was longer than during level locomotion. This observation is supported by the slightly more extended hip and knee joints during stance, and a stiffer INT joint (less flexion–extension than level locomotion for assumed similar ground reaction forces), which might also have induced a vaulting descending motion of the CoM towards the lowered substrate.

To cope with visible drops of 50% leg length, the trailing leg displayed a more crouched configuration, and was less retracted than during level locomotion (Fig. 2H). The shorter effective leg was produced by a significantly more flexed hip, INT and knee joints. Leg retraction displayed a trade-off between flexion of the hip, which protracted the leg, and of the knee, which in turn induced the contrary motion.

Thus, the quail used a large hip extension to extend the effective leg during stance but did not use a larger hip flexion to shorten it. This can be explained by the fact that hip extensor torque must be sufficient to stabilize a pronograde trunk and the overall locomotion[22,40,47].

At TD and during later stance, the trailing whole leg was nearly vertically oriented for 25% and 50% visible drops. Such a leg orientation may help to prevent a collapse of the leg. For the largest drop, the hip was significantly more abducted (see Fig. 4K). The described leg placement permitted the pelvis to be rotated towards the trailing leg (yaw motion) and tilted towards the leading leg (roll motion) while descending towards the lowered substrate (Fig. 4E,F).

Leading limb (stride i). The leading effective leg touched down significantly later when stepping down, if compared to the same event during level locomotion. The angle of attack (α_0) was steeper but did not vary with drop-height. At the same time, the retraction of the trailing limb in the late stance was step-height related. This indicates that leading leg retraction was decoupled from the trailing leg after crossing to the ground level, as observed in the change of the aperture angle (ϕ_0) (see Fig. 2J). This result suggests that the angle of attack and not the aperture angle is a target control parameter for leg placement when negotiating visible drops.

During 1 cm drops, the effective leg lengthening during swing is explained by hip extension, but especially by the significant extension of the TMP joint before TD. This shaped the subsequent behavior of the leg during stance. We think that the more extended TMP joint at TD shifted spring-like behavior from the INT to the TMP joint (cp. Fig. 3J,L, green lines after TD). Note that this behavior is similar to the "KEh-mode" observed during an unexpected drop, in which the drop energy is converted to horizontal kinetic energy, see[44]. Gordon and colleagues showed that the guinea fowl displayed significantly higher activation of the *M. flexor perforatus digiti III* before and after their leg touched down in a sunken substrate[8]. We speculate, that by preloading the tendons spanning the TMP joint during swing, the quail changed the viscoelastic properties of the joint (i.e., they shifted from a more damped joint behavior dominated by muscle properties to a more spring-like behavior dominated by elastic tissues, as observed in running humans[52] and turkeys[53]. The consequences of this change for joint control goals like minimization of joint work[54] needs further investigation.

As was observed for drops of 10% leg length, the quail used a more extended leading leg (stride i) to negotiate drops of 25% leg length compared to level or 5 cm drops (see Table S1). However, the source of the leading leg lengthening was different from those depicted for drops of 10% leg length. The quail extended the INT joint instead of the TMP joint during swing (see Fig. 3J,L red curves). This simple change effected a dampened leg response after the drop. Focusing on the joint level, the TMP joint abandoned the spring-like behavior during stance depicted during 10% drops, and exhibited the dampened pattern described for level locomotion[3]. It seems that the extension of the INT joint during swing permits muscular work to control leg compression and thus the energy dissipation after a visible drop. EMG data from the guinea fowl negotiating slow drops showed that the *M. gastrocnemius pars lateralis* was recruited earlier than the *M. flexores perforate digiti* III. This shift in the activation vanished for faster drops and level locomotion[9]. Perhaps the onset in the activation of these muscles is used by birds to shape the viscoelastic response of the leg.

To negotiate 50% leg length drops, the aperture angle between the effective legs was similar to 25% leg length drops until the level line. However, after the leg crossed the level height, it was extended until TD. Note that the slope of the mean leg angle before TD was quite flat until the level line (Fig. 2J blue line). Consequently, the retraction speed of the leading leg was only slightly adapted when level TD is lost (Fig. 2J blue dotted line). At TD, the leading effective leg was shorter than in other drop conditions. Distal joint angles during 50% leg length drops were not significantly different from those exhibited by 2.5 cm drops. During this rather cautious drop negotiating technique, leg shortening seems to be performed by a more flexed hip joint at TD. During stance, the INT displayed a more bouncing-like behavior.

With increased drop height, the whole leg was more vertically oriented in the frontal plane and less abducted in the lowered substrate compared to unrestricted locomotion. This leg placement strategy prevented leg collapse and might have permitted the reorientation of the pelvis and thus the trunk in motion's direction.

Conclusions

To negotiate visible steps, the quail reconfigured leg and joint kinematics related to step type (upwards vs. downwards) and height via different anticipatory strategies during swing and/or reactive control after TD. However, dramatic changes were observed only in the trailing limb for step heights of 50% of leg length. Leg and joint adaptations permitted the quail to regain steady-state locomotion already after one or two steps.

When coping with steps upwards, the quail adapted the trailing limb to permit that the leading leg steps on the elevated substrate in the same way as it does during level locomotion. This strategy may have reduced the need of reactive (feedback) response to readapt posture during leading leg's stance.

The quail kept the kinematic patterns of the distal joints to a large extent unchanged during uneven locomotion, and most changes were accomplished in proximal joints. Up to middle step heights, hip extension was mainly used to lengthen the leg, or in combination with a more spring-like TMP joint to change to aerial running. However, to negotiate the largest visible step upwards and drop heights, all joints contributed to leg lengthening/shortening in the trailing leg and both the trailing and leading legs stepped more vertically and less abducted. This indicates a sudden change in leg motor-control program. Further analysis is certainly necessary to understand

Individual	Weight (g)	Strides					
		1 cm up	2.5 cm up	5 cm up	1 cm down	2.5 cm down	5 cm down
Schwarz	341		1	5	1	5	2
Rot	284		3	4		4	1
Silber	295	1	5	2	2	2	
Dunkelgrün	337	4	2	3	2	1	3
Hellgrün	277		3				
Lila	362	1					
Rosa	342						
Orange	295			2			
Gelb	307	3	2			4	3

Table 2. Animals and strides.

muscle synergies, and overall neuromechanics underlining changes between "dynamical" (spinal controlled) and more "safely" (slower, goal-directed motions, perhaps from higher centers controlled) gait programs.

Methods

Animals. Nine adult common quails [Phasianidae: *Coturnix coturnix* (Linnaeus 1758)] displaying a mean body weight 315 ± 30 g were used for our analysis (see Table 2). The birds were housed at the Institute of Zoology and Evolutionary Research in Jena with access to food and water ad libitum. Housing, care, and all experimental procedures were approved by the Committee for Animal Research of the State of Thuringia (registry number 02-054/14). Animal keeping and experiments were performed in strictly accordance with the approved guidelines.

Experiments. For information about level locomotion experiments, please refer to[3]. In the step-up/step-down experiments, the quails moved across a 3 m long walking track at their preferred speeds. In the middle of the walking track, the birds negotiated visible drop/step-up conditions of 1.0 cm, 2.5 cm, and 5 cm. Those challenges were created by supplementing the first (for drops) or the last (for step-up) half of the walking track. The track was covered with fine sheet rubber to reduce slipping. Body and limb kinematics were collected by using a biplanar X-ray fluoroscope (Neurostar, Siemens, Erlangen, Germany) at the facility of the Institute of Zoology and Evolutionary Research, Germany. X-ray sources were set to obtain recordings from the laterolateral and ventrodorsal projections. In addition, two synchronized standard light high-speed cameras (SpeedCam Visario g2, Weinberger, Erlangen, Germany) were used to cover both frontal and lateral perspectives of the track. The X-ray machine parameters were 40 kV and 53 mA, and a sampling frequency of 500 Hz. Raw video data was first undistorted by using a modified version of the freely available MATLAB (The MathWorks, Natick, MA, USA) routine batchUndistort (www.xromm.org) provided by Brown University (Providence, RI, USA). As a base for the Automatic Anatomical Landmark Localization using Deep Features (see below), manual digitization of the joints and other landmarks [following[3]] was performed using SimiMotion software (SimiMotion Systems, Unterschleißheim, Germany) on no more than ten randomly distributed frames per trial. Note that 5–10 annotated frame pairs are sufficient to train a model with the same annotation performance as manual landmark labeling[55,56].

Automatic anatomical landmark localization in multi-view sequences using deep features. In the following, the automatic multi-view landmark localization technique of the locomotion sequence is described, which is originally published in[57]. Our method utilizes multi-view deep concatenated feature representations of annotated input images to train individual linear regressors for each view-based correspondent landmark pair. Based on a small number of annotated correspondent images of a multi-view sequence, the individual trained regressors locate all landmarks of the entire sequence in each view. In Fig. 6 the whole method pipeline is visualized. Afterwards, the automatic localized 2D landmarks of the dorsoventral and lateral view are utilized to reconstruct 3D landmark coordinates.

The utilized deep features are learned representations of images extracted from a Convolutional Neural Network (CNN)[58], which are mainly used for supervised computer vision tasks, like image classification, object recognition, or object tracking. The CNN learn in each of its convolutional layer several sets of individual convolutional filters based on the input images in the training process and provides thereby powerful feature representations of the utilized image domain.

The training of CNN models usually needs a lot of data, which is not available in our application. Hence, we choose a model of the AlexNet architecture[59] pre-trained on a similar task exploiting the same data domain of our application. This pre-trained model is trained for pose classification with the very same data of multi-view bipedal locomotion sequences to distinguish 10 quantized poses in each view. The semi-automatic annotation of the poses is described in[57]. After training the CNN on the auxiliary task of pose classification, the CNN's layer activations during inference can be exploited as deep features. In the following, we describe the regressor training process for a single two-view locomotion sequence S utilizing the deep features.

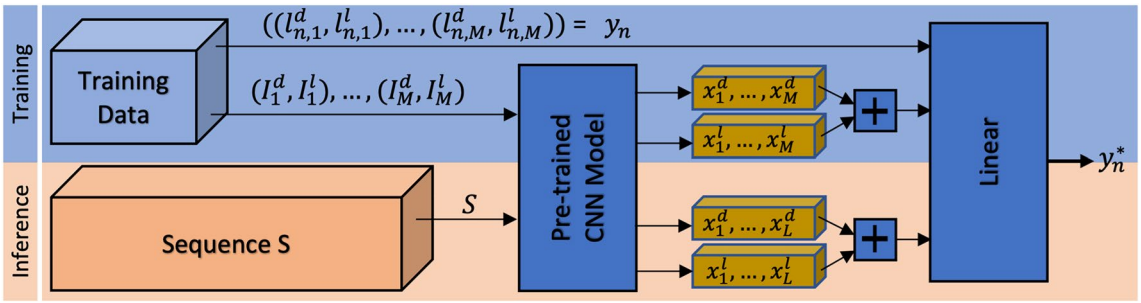

Figure 6. To train an individual multi-view landmark regressor h_n, initially, the deep features $x_i = ((x_1^d, \ldots, x_M^d, x_1^l, \ldots, x_M^l)$ are extracted of M annotated image pairs. Afterwards, the concatenated features of correspondent image pairs serve as input for the regressor training. The landmark positions y_n^* of unseen image pairs of S are predicted from the resulting trained model h_n. This procedure is repeated for each of the N landmark pairs individually.

The multi-view locomotion sequence S contains L correspondent image pairs from the dorsoventral and lateral view $(I_1^d, \ldots, I_L^d)$ and $(I_1^l, \ldots, I_L^l)$. From each image pair I_i^d and I_i^l the deep features $x_i = (x_i^l, x_i^d)$ are extracted and concatenated from the fifth convolutional layer Conv-5 of the pre-trained CNN. Additionally, in $M = 10$ equidistant sampled frame pairs of both views, the correspondent $N = 22$ landmark position pairs $y_n = (y_1, \ldots, y_N)$ with $y_n = ((l_{n,1}^d, l_{n,1}^l), \ldots, (l_{n,M}^d, l_{n,M}^l))$ are annotated, which are used for single regressor training.

By utilizing each annotated corresponding landmark pairs y_n, individual linear regressors h_n are trained, which locates the correspondent landmarks in the remaining $L - M$ images of both views, automatically.

As linear model h_n, we train N single ϵ-SV regressors[60]. Each linear regression model h_n uses the given training data $(x_1, y_1), \ldots, (x_M, y_N) \subset X \times R$, where x_i denotes the deep features with $X \times R^D$ and y_i the landmark positions of the ith landmark in the M frames. Hence, for each landmark position pair of both views, a single regressor h_i is trained.

The goal of this regression task is to find a hyperplane $f(x) = \langle \omega, x \rangle + b$ with a maximum deviation of ϵ from the target values y_i for all training data. Given the fact that the vector ω is perpendicular to the hyperplane $f(x)$, we only need to minimize the norm of ω, i.e.,$\|\omega\|^2 = \langle \omega, \omega \rangle$. When working with real data, in most cases, it is impossible to find a decent solution for this convex optimization problem based on potential outliers. With the addition of slack variables $\xi_i and \xi_i^*$ such infeasible conditions can be handled. We formulate the problem like[51]:

$$\frac{1}{2}\|\omega\|^2 + C\sum_{i=1}^{L}(\xi_i + \xi_i^*)$$

$$s.t.\{y_i - \langle \omega, x_i \rangle - b \leq \epsilon + \xi_i \langle \omega, x_i \rangle + b - y_i \leq \epsilon + \xi_i^* \xi_i, \xi_i^* \geq 0,$$

where $C > 0$ is a constant, which weights the tolerance of deviation greater than ϵ.

Multi-view 3D reconstruction. The dorsoventral and lateral two-dimensional position data can be exploited to reconstruct these corresponded landmark points to three-dimensional points in a metric space. For this, a three-dimensional calibration cube was used to perform the 3D reconstruction process. The cube is semi-transparent and contains equidistant X-ray opaque metal spheres. By annotating at least seven individual corresponding spheres in both views, a relationship between the *annotated 2D pixel position* $((u_i^d, v_i^d), (u_i^l, v_i^l))$ *to the 3D real word positions* (X_i, Y_i, Z_i) *of* the spheres can be exploited. For more details on how P is estimated, we refer to[61].

Angle calculation. Joint angles were computed as explained in[3], while model related leg kinematics following[22,62].

Three-dimensional kinematics (see Fig. 1D): the pelvic local coordinate system was located in the centroid of the triangle composed by both hip joints and the pelvis cranial marker (p_c). It measures the absolute motion of the pelvis related to the global coordinate system. It was defined by specifying first $\vec{e}_{x-int_{pel}}$ as an interim vector pointing from the right hip joint (h_r) to the pelvis cranial marker $\vec{e}_{x-int_{pel}} = p_c - h_r$, then $\vec{e}_{y_{pel}}$ to be a vector pointing from $h_r$to the left hip joint (h_l), $\vec{e}_{y_{pel}} = h_l - h_r$, and $\vec{e}_{z_{pel}}$ and $\vec{e}_{x_{pel}}$ via cross-products as $\vec{e}_{z_{pel}} = \vec{e}_{x-int_{pel}} \times \vec{e}_{y_{pel}}$ and $\vec{e}_{x_{pel}} = \vec{e}_{y_{pel}} \times \vec{e}_{z_{pel}}$. The whole-leg coordinate system measures the rotation of the whole leg related to the pelvis (estimates the three-dimensional rotations occurring at the hip joint). It was constructed as follows: $\vec{e}_{z_{leg\_i}}$ extends from the knee joint (k_i) to the hip joint h_i (right leg, $_{i=r}$, left leg, $_{i=l}$), e.g. $\vec{e}_{z_{leg\_i}} = h_i - k_i$. Then $\vec{e}_{x-int_{leg\_i}}$ is an interim vector directed from TMP-distal markers (tmp_{dist_i}) to k_i, e.g., $\vec{e}_{x-int_{leg\_i}} = k_i - tmp_{dist\_i}$. $\vec{e}_{y_{leg\_i}}$ was then obtained as $\vec{e}_{y_{leg\_i}} = \vec{e}_{z_{leg\_i}} \times \vec{e}_{x-int_{leg\_i}}$, $\vec{e}_{y_{leg\_i}}$ is hence perpendicular to the plane defined by the hip joint, the knee joint and the TMP-distal marker and points to the left (towards medial for the right leg and lateral for the left leg). Finally, $\vec{e}_{x_{leg\_i}} = \vec{e}_{y_{leg\_i}} \times \vec{e}_{z_{leg\_i}}$. The whole-leg coordinate system was located in the middle of the femur (segment between hip and knee). To compute three-dimensional angles, we used the Cardan rotation sequence z–x–y. The left leg was used as reference. Thus, positive rotations around the x, y, and z axes represent, respectively, the inner rotation of the femur (whole leg

rotates laterally), femoral retraction (hip extension), and femoral abduction. To build the mean using both legs, rotations around the z and x axes for the right leg were multiplied by − 1. Because of the constrained field of view, events defining a stride were selected in a different way for the leading and the trailing limbs. For the trailing limb the stride was defined between TD on the level plate and TD on the vertical shifted plate. For the leading limb between TO on the level plate and TO on the vertical shifted plate. For comparison, strides were afterwards interpolated to 100 points. Kinematics were computed using a custom written script in Matlab 2017 (The MathWorks Inc., Natick, MA, USA).

Statistical analysis. The following kinematic variables were defined as dependent variables: global parameters such as angle of attack (α_0), aperture angle (ϕ_0) and leg length (l), effective leg axial velocity ($\dot{l}$), effective leg angle velocity ($\dot{\alpha}$), aperture angle velocity ($\dot{\phi}$), all joint angles and cardan angles for the pelvis and hip joint (relative angles between pelvis and leg, see Figs. 1, 2, 3, 4 and 5). For the trailing limb, we analyzed the early stance (15%, because at TD in most cases data was absent) and TO events. For the leading limb, we analyzed the TD and the late stance (85%). In our analysis, we also included the four precedents and the four following points relative to the selected event (event ± 4% of the stride).

Step locomotion are paired measures (same individuals, comparison between the i-1 and the i events) while step vs. level locomotion (grounded running) unpaired [level locomotion was collected in a different study[3]]. For step locomotion, repeated measures ANOVA was used to assess the influence of step-height and direction (up vs. drop) to the dependent variables. To test for significant differences between each step condition and level locomotion, we performed single multivariate ANOVAs (e.g., 2.5 cm step upwards vs. level). Post-Hoc were afterwards performed to assess the influence of each treatment. Based on the homogeneity of the variances (Levene-test) we selected between TukeyHSD or Games–Howell tests.

Statistical analysis was implemented in R (Version: 3.5.3). We used the following libraries (R.matlab, data.table, stats, rstatix und car). To generate R-code we used the program "master" (free downloadable under https://starkrats.de).

Ethics approval and consent to participate. All experiments were approved by and carried out in strict accordance with the German Animal Welfare guidelines and regulations of the states of Thuringia (TLV 02-054/14). We confirm that we complied with the ARRIVE guidelines.

Data availability

The datasets used and/or analyzed during the current study are available from the corresponding author on reasonable request.

Received: 27 January 2022; Accepted: 12 September 2022
Published online: 23 September 2022

References

1. Kilbourne, B. M., Andrada, E., Fischer, M. S. & Nyakatura, J. A. Morphology and motion: Hindlimb proportions and swing phase kinematics in terrestrially locomoting charadriiform birds. *J. Exp. Biol.* **219**, 1405–1416 (2016).
2. Nyakatura, J. A., Andrada, E., Grimm, N., Weise, H. & Fischer, M. S. Kinematics and center of mass mechanics during terrestrial locomotion in Northern Lapwings (Vanellus vanellus, Charadriiformes). *J. Exp. Zool. Part A Ecol. Genet. Physiol.* **317**, 580–594. https://doi.org/10.1002/jez.1750 (2012).
3. Andrada, E., Nyakatura, J. A., Bergmann, F. & Blickhan, R. Adjustments of global and local hindlimb properties during terrestrial locomotion of the common quail (*Coturnix coturnix*). *J. Exp. Biol.* **216**, 3906–3916 (2013).
4. Andrada, E., Rode, C. & Blickhan, R. Grounded running in quails: Simulations indicate benefits of observed fixed aperture angle between legs before touch-down. *J. Theor. Biol.* **335**, 97–107 (2013).
5. Blickhan, R. *et al.* Intelligence by mechanics. *Philos. Trans. A Math. Phys. Eng. Sci.* **365**, 199–220. https://doi.org/10.1098/rsta.2006.1911 (2007).
6. Gordon, M. S., Blickhan, R., Dabiri, J. O. & Videler, J. J. *Animal Locomotion: Physical Principles and Adaptations* (CRC Press, 2017).
7. Dickinson, M. H. *et al.* How animals move: An integrative view. *Science* **288**, 100–106 (2000).
8. Nishikawa, K. *et al.* Neuromechanics: An integrative approach for understanding motor control. *Integr. Comp. Biol.* **47**, 16–54. https://doi.org/10.1093/icb/icm024 (2007).
9. Gordon, J. C., Rankin, J. W. & Daley, M. A. How do treadmill speed and terrain visibility influence neuromuscular control of guinea fowl locomotion?. *J. Exp. Biol.* **218**, 3010–3022 (2015).
10. Farley, C. T., Houdijk, H. H. P., Van Strien, C. & Louie, M. Mechanism of leg stiffness adjustment for hopping on surfaces of different stiffnesses. *J. Appl. Physiol.* **85**, 1044–1055 (1998).
11. Ferris, D. P., Liang, K. & Farley, C. T. Runners adjust leg stiffness for their first step on a new running surface. *J. Biomech.* **32**, 787–794. https://doi.org/10.1016/S0021-9290(99)00078-0 (1999).
12. Muller, R. & Blickhan, R. Running on uneven ground: Leg adjustments to altered ground level. *Hum. Mov. Sci.* **29**, 578–589. https://doi.org/10.1016/j.humov.2010.04.007 (2010).
13. Müller, R., Tschiesche, K. & Blickhan, R. Kinetic and kinematic adjustments during perturbed walking across visible and camouflaged drops in ground level. *J. Biomech.* **47**, 2286–2291 (2014).
14. Birn-Jeffery, A. V. & Daley, M. A. Birds achieve high robustness in uneven terrain through active control of landing conditions. *J. Exp. Biol.* **215**, 2117–2127. https://doi.org/10.1242/jeb.065557 (2012).
15. Birn-Jeffery, A. V. *et al.* Don't break a leg: Running birds from quail to ostrich prioritise leg safety and economy on uneven terrain. *J. Exp. Biol.* **217**, 3786–3796 (2014).
16. Seyfarth, A., Geyer, H. & Herr, H. Swing-leg retraction: A simple control model for stable running. *J. Exp. Biol.* **206**, 2547–2555 (2003).
17. Daley, M. A., Usherwood, J. R., Felix, G. & Biewener, A. A. Running over rough terrain: Guinea fowl maintain dynamic stability despite a large unexpected change in substrate height. *J. Exp. Biol.* **209**, 171–187. https://doi.org/10.1242/jeb.01986 (2006).
18. Blum, Y. *et al.* Swing-leg trajectory of running guinea fowl suggests task-level priority of force regulation rather than disturbance rejection. *PLoS ONE* **9**, e100399 (2014).

19. Blum, Y., Birn-Jeffery, A., Daley, M. A. & Seyfarth, A. Does a crouched leg posture enhance running stability and robustness?. *J. Theor. Biol.* **281**, 97–106. https://doi.org/10.1016/j.jtbi.2011.04.029 (2011).
20. Daley, M. A. & Usherwood, J. R. Two explanations for the compliant running paradox: Reduced work of bouncing viscera and increased stability in uneven terrain. *Biol. Lett.* **6**, 418–421. https://doi.org/10.1098/rsbl.2010.0175 (2010).
21. Andrada, E., Blickhan, R., Ogihara, N. & Rode, C. Low leg compliance permits grounded running at speeds where the inverted pendulum model gets airborne. *J. Theoret. Biol.* **110227**, 25 (2020).
22. Andrada, E., Rode, C., Sutedja, Y., Nyakatura, J. A. & Blickhan, R. Trunk orientation causes asymmetries in leg function in small bird terrestrial locomotion. *Proc R. Soc. B Biol. Sci.* https://doi.org/10.1098/rspb.2014.1405 (2014).
23. Müller, R. & Andrada, E. Skipping on uneven ground: Trailing leg adjustments simplify control and enhance robustness. *R. Soc. Open Sci.* **5**, 172114 (2018).
24. Andrada, E. *et al.* Mixed gaits in small avian terrestrial locomotion. *Sci. Rep.* **5**, 13636. https://doi.org/10.1038/srep13636 (2015).
25. Abourachid, A. *et al.* Bird terrestrial locomotion as revealed by 3D kinematics. *Zoology* **114**, 360–368. https://doi.org/10.1016/j.zool.2011.07.002 (2011).
26. Kambic, R. E., Roberts, T. J. & Gatesy, S. M. Long-axis rotation: A missing degree of freedom in avian bipedal locomotion. *J. Exp. Biol.* **217**, 2770–2782. https://doi.org/10.1242/jeb.101428 (2014).
27. Rubenson, J., Lloyd, D. G., Besier, T. F., Heliams, D. B. & Fournier, P. A. Running in ostriches (*Struthio camelus*): Three-dimensional joint axes alignment and joint kinematics. *J. Exp. Biol.* **210**, 2548–2562 (2007).
28. Kambic, R. E., Roberts, T. J. & Gatesy, S. M. Guineafowl with a twist: Asymmetric limb control in steady bipedal locomotion. *J. Exp. Biol.* **218**, 3836–3844 (2015).
29. Blickhan, R. The spring-mass model for running and hopping. *J. Biomech.* **22**, 1217–1227. https://doi.org/10.1016/0021-9290(89)90224-8 (1989).
30. Ruina, A., Bertram, J. E. & Srinivasan, M. A collisional model of the energetic cost of support work qualitatively explains leg sequencing in walking and galloping, pseudo-elastic leg behavior in running and the walk-to-run transition. *J. Theor. Biol.* **237**, 170–192 (2005).
31. Srinivasan, M. & Ruina, A. Computer optimization of a minimal biped model discovers walking and running. *Nature* **439**, 72–75 (2006).
32. Full, R. J. & Koditschek, D. E. Templates and anchors: Neuromechanical hypotheses of legged locomotion on land. *J. Exp. Biol.* **202**, 3325–3332 (1999).
33. Ogihara, N., Kikuchi, T., Ishiguro, Y., Makishima, H. & Nakatsukasa, M. Planar covariation of limb elevation angles during bipedal walking in the Japanese macaque. *J. R. Soc. Interface* **9**, 2181–2190 (2012).
34. Ogihara, N. *et al.* Planar covariation of limb elevation angles during bipedal locomotion in common quails (*Coturnix coturnix*). *J. Exp. Biol.* **217**, 3968–3973 (2014).
35. Ivanenko, Y. P., Cappellini, G., Dominici, N., Poppele, R. E. & Lacquaniti, F. Modular control of limb movements during human locomotion. *J. Neurosci.* **27**, 11149–11161 (2007).
36. Ivanenko, Y. P., d'Avella, A., Poppele, R. E. & Lacquaniti, F. On the origin of planar covariation of elevation angles during human locomotion. *J. Neurophysiol.* **99**, 1890–1898 (2008).
37. Borghese, N., Bianchi, L. & Lacquaniti, F. Kinematic determinants of human locomotion. *J. Physiol.* **494**, 863 (1996).
38. Daley, M. A. In *9th International Symposium on Adaptive Motion of Animals and Machines (AMAM 2019).*
39. Beebe, W. *The Bird: Its Form and Function* Vol. 1 (Henry Holt and Company, 1906).
40. Maus, H. M., Lipfert, S. W., Gross, M., Rummel, J. & Seyfarth, A. Upright human gait did not provide a major mechanical challenge for our ancestors. *Nat. Commun.* **1**, 70. https://doi.org/10.1038/ncomms1073 (2010).
41. Blickhan, R., Ernst, M., Koch, M. & Müller, R. Coping with disturbances. *Hum. Mov. Sci.* **32**, 971–983 (2013).
42. Ernst, M., Götze, M., Müller, R. & Blickhan, R. Vertical adaptation of the center of mass in human running on uneven ground. *Hum. Mov. Sci.* **38**, 293–304 (2014).
43. Müller, R., Ernst, M. & Blickhan, R. Leg adjustments during running across visible and camouflaged incidental changes in ground level. *J. Exp. Biol.* **215**, 3072–3079. https://doi.org/10.1242/jeb.072314 (2012).
44. Daley, M. A., Felix, G. & Biewener, A. A. Running stability is enhanced by a proximo-distal gradient in joint neuromechanical control. *J. Exp. Biol.* **210**, 383–394. https://doi.org/10.1242/jeb.02668 (2007).
45. Blickhan, R., Andrada, E., Müller, R., Rode, C. & Ogihara, N. Positioning the hip with respect to the COM: Consequences for leg operation. *J. Theor. Biol.* **382**, 187–197. https://doi.org/10.1016/j.jtbi.2015.06.036 (2015).
46. Gunther, M., Keppler, V., Seyfarth, A. & Blickhan, R. Human leg design: Optimal axial alignment under constraints. *J. Math. Biol.* **48**, 623–646. https://doi.org/10.1007/s00285-004-0269-3 (2004).
47. Shen, Z. H. & Seipel, J. E. A fundamental mechanism of legged locomotion with hip torque and leg damping. *Bioinspir. Biomim.* **7**, 046010 (2012).
48. Witte, H. *et al.* In *Proceedings of CLAWAR'2001–4th International Conference on Climbing and Walking Robots.* 63–68.
49. Witte, H. *et al.* In *International Symposium on Adaptive Motion of Animals and Machines.*
50. Daley, M. A. & Biewener, A. A. Leg muscles that mediate stability: Mechanics and control of two distal extensor muscles during obstacle negotiation in the guinea fowl. *Philos. Trans. R. Soc. B Biol. Sci.* **366**, 1580–1591 (2011).
51. Jindrich, D. L. & Full, R. J. Dynamic stabilization of rapid hexapedal locomotion. *J. Exp. Biol.* **205**, 2803–2823 (2002).
52. Farris, D. J. & Sawicki, G. S. Human medial gastrocnemius force–velocity behavior shifts with locomotion speed and gait. *Proc. Natl. Acad. Sci.* **109**, 977–982 (2012).
53. Roberts, T. J., Marsh, R. L., Weyand, P. G. & Taylor, C. R. Muscular force in running turkeys: The economy of minimizing work. *Science* **275**, 1113–1115 (1997).
54. Rode, C., Sutedja, Y., Kilbourne, B. M., Blickhan, R. & Andrada, E. Minimizing the cost of locomotion with inclined trunk predicts crouched leg kinematics of small birds at realistic levels of elastic recoil. *J. Exp. Biol.* **219**, 485–490 (2016).
55. Haase, D., Nyakatura, J. & Denzler, J. Comparative large-scale evaluation of human and active appearance model based tracking performance of anatomical landmarks in X-ray locomotion sequences. *Pattern Recogn. Image Anal.* **24**, 86–92 (2014).
56. Haase, D., Nyakatura, J. A. & Denzler, J. In *Joint Pattern Recognition Symposium.* 11–20 (Springer).
57. Mothes, O. & Denzler, J. In International Conference on Pattern Recognition (ICPR)—VAIB workshop (2018).
58. Goodfellow, I., Bengio, Y. & Courville, A. *Deep Learning* (MIT Press, 2016).
59. Krizhevsky, A., Sutskever, I. & Hinton, G. E. Imagenet classification with deep convolutional neural networks. *Adv. Neural. Inf. Process. Syst.* **25**, 1097–1105 (2012).
60. Vapnik, V. *The Nature of Statistical Learning Theory* (Springer, 1999).
61. Gonzalez, R. C. & Woods, R. E. *Digital Image Processing* 4th edn. (Pearson, 2018).
62. Blickhan, R., Andrada, E., Hirasaki, E. & Ogihara, N. Global dynamics of bipedal macaques during grounded and aerial running. *J. Exp. Biol.* **221**, 58 (2018).

Acknowledgements

We would like to thank Lisa Dargel for animal training and animal guidance during the experiments. Rommy Petersohn and Yefta Sutedja for their technical assistance during the experiments. Ben Witt (formerly known as

Ben Derwel) together with students worked hard to digitalize landmarks from the X-ray images for the semi-automatic identification.

Author contributions

E.A., M.S.F., and R.B. conceived the study. E.A. and M.S.F. supervised the experiments. J.D. and O.M. developed and O.M. performed the semi-automatic landmark identification, E.A. analyzed experimental data inclusive 2D and 3D kinematics, H.S. performed the statistics, E.A., M.S.F., D.J., M.T. and R.B. grants acquisition. E.A. drafted the manuscript. All authors contributed to the interpretation of the results and revised the manuscript.

Funding

Open Access funding enabled and organized by Projekt DEAL. The study was supported by the German Research Foundation DFG-grants (De 735/8-1/3, Bl 236/22-1/3, Fi 410/15-1/3, AN 1286/2-1) to DJ, RB, MSF and EA, respectively. This work was also supported by DFG FI 410/16-1 and NSF (DBI-2015317) as part of the NSF/CIHR/DFG/FRQ/UKRI-MRC Next Generation Networks for Neuroscience Program.

Competing interests

The authors declare no competing interests.

Additional information

Supplementary Information The online version contains supplementary material available at https://doi.org/10.1038/s41598-022-20247-y.

Correspondence and requests for materials should be addressed to E.A.

Reprints and permissions information is available at www.nature.com/reprints.

Publisher's note Springer Nature remains neutral with regard to jurisdictional claims in published maps and institutional affiliations.